Structural properties and fragile to strong transition in confined water

M. De Marzio, G. Camisasca, M. M. Conde, M. Rovere, and P. Gallo

Citation: The Journal of Chemical Physics **146**, 084505 (2017); doi: 10.1063/1.4975624
View online: http://dx.doi.org/10.1063/1.4975624
View Table of Contents: http://aip.scitation.org/toc/jcp/146/8
Published by the American Institute of Physics

Structural properties and fragile to strong transition in confined water

M. De Marzio, G. Camisasca, M. M. Conde, M. Rovere, and P. Gallo
Dipartimento di Matematica e Fisica, Università "Roma Tre," Via della Vasca Navale 84, 00146 Roma, Italy

(Received 13 October 2016; accepted 22 January 2017; published online 28 February 2017)

We derive by computer simulation the radial distribution functions of water confined in a silica pore modeled to reproduce MCM-41. We perform the calculations in a range of temperatures from ambient to deep supercooling for the subset of water molecules that reside in the inner shell (free water) by applying the excluded volume corrections. By comparing with bulk water we find that the first shell of the oxygen-oxygen and hydrogen-hydrogen radial distribution functions is less sharp and the first minimum fills in while the oxygen-hydrogen structure does not significantly change, indicating that the free water keeps the hydrogen bond short range order. The two body excess entropy of supercooled water is calculated from the radial distribution functions. We connect the behavior of this function to the relaxation time of the same system already studied in previous simulations. We show that the two body entropy changes its behavior in coincidence with the crossover of the relaxation time from the mode coupling fragile to the strong Arrhenius regime. As for bulk water also in confinement, the two body entropy has a strict connection with the dynamical relaxation. *Published by AIP Publishing.* [http://dx.doi.org/10.1063/1.4975624]

I. INTRODUCTION

The study of confined water is of relevant interest for the connection with phenomena in chemistry, biology, and technological applications. On one side the focus is on the role of water in chemical and biological processes,[1] on the other side numerous studies investigate how the interaction with substrates could modify the properties of liquid water.[2,3] This last issue has become particularly relevant in connection with the recent debate about the existence of a liquid-liquid critical point (LLCP) in supercooled water. A large amount of experimental and computer simulation work has been devoted to the study of the LLCP.[2,4–10] The presence of a coexistence line between a low density liquid (LDL) phase and a high density liquid (HDL) phase of water terminating in a critical point could explain a number of thermodynamic anomalies of this liquid in the metastable supercooled state.[11,12] The LDL and HDL phases would present differences in the structures in analogy with the corresponding glassy states of the low density amorphous (LDA) and the high density amorphous (HDA) ices.[13–16] Rigorous proofs of the existence and second order nature of the LLCP are found for ST2 and Jagla water in computer simulations implemented with studies of free energy and scaling properties.[17–20] In experiments however the homogeneous nucleation makes very difficult a direct observation of the LLCP in the so-called *no-man's land*.[21–23] New experimental techniques recently opened the possibility of partially exploring the no-man's land in bulk water.[24] Nonetheless in confined water it is easier to study experimentally the supercooled region avoiding crystallization provided that confined water behaves similarly to the bulk.

In computer simulations, dynamical properties of supercooled water have also been largely explored. It was discovered for bulk SPC/E water[25,26] that the dynamics of supercooled water can be interpreted in the framework of the Mode Coupling Theory (MCT) of glassy dynamics.[27] In the mild supercooled region the α relaxation time increases with decreasing temperature with a power law and apparently diverges at a critical MCT temperature T_C. This divergence at T_C is determined by the ideal transition from an ergodic to a non-ergodic regime. The interpretation in terms of MCT in this region was also confirmed in experiments.[28,29]

In the deep supercooled region, however, the MCT transition is prevented by the appearance of hopping effects.[30] As a consequence on approaching T_C the relaxation time deviates from the MCT behavior. At a temperature $T_L > T_C$ the relaxation time starts to increase with an Arrhenius behavior typical of activated processes. T_L can be assumed as the temperature of a fragile to strong crossover (FSC). From quasi-elastic neutron scattering (QENS) on water confined in MCM-41 the occurrence of a FSC was found[31–33] and it was also evidenced that the FSC line as a function of pressure approaches the location of the LLCP predicted in bulk water by extrapolation of experimental data.[22,23] This behavior has been also found in a number of computer simulations with different models for bulk water and aqueous solutions.[34–39] The FSC has been detected to take place for water at the crossing of the so-called Widom line, e.g., the locus of maxima of the correlation length, emanating from the LLCP in the one phase region.[35,40,41] This implies a strong connection between thermodynamics and dynamical behavior. The important role of hopping processes in determining the fragile to strong transition and the connection to the Widom line has been explored in detail recently for bulk water.[30]

Being confined water possibly different from bulk water experiments on water in MCM-41 needed a microscopic study to test if bulk-like properties could be explored in such a sample. Indeed a computer simulation of SPC/E water embedded in a model of MCM-41[42–44] showed that this was the case.

It was evident from this simulation that water in contact with the hydrophilic substrate suffers a layering effect with the formation of a double layer of almost immobile molecules. This bound water resides on average in a range of circa 0.3 nm from the confining surface and it is not detected in QENS experiments. The water in the layer close to center of the pore (free water) is more mobile and it was found to behave like bulk water upon cooling. In particular it was found that the dynamics of confined free water can be interpreted in the framework of the MCT like in glass formers upon confinement.[45] Moreover in agreement with experiments a FSC[42,43] was found at a temperature $T_L \approx 215$ K. T_L also coincides with a maximum in the specific heat indicating the connection between dynamics and thermodynamics.

In this paper we explore the relation between structure, thermodynamics, and dynamics in confined water by considering the radial distribution functions (RDFs) and the two body entropy derived from the RDF.

At variance with the bulk, the calculation of the RDF in confined geometries requires taking into account the finite volume effects. Moreover in our system the water molecules are confined in a cylindrical geometry with a rough surface. For these reasons we consider the procedure used for a similar calculation for water confined in a larger pore, a Vycor pore,[46,47] and we adapt that procedure to the case of MCM-41 that has a more restricted volume.

We present in this paper the calculation of the site-site RDF for the free part of the confined water upon cooling and compare it with the SPC/E bulk RDFs.

From the RDF we can derive the two body excess entropy and explore how its behavior upon supercooling can be connected to the MCT.

The idea of relating diffusion in a fluid to the excess entropy goes back to Rosenfeld.[48–50] The excess entropy is determined by the particle interaction and it becomes more negative at decreasing temperature to partially compensate the ideal gas contribution. The diffusion process must be correlated with the accessible configurations that are estimated by the excess entropy. The empirical relationships between the diffusion constant and the excess entropy are based on the assumption

$$D \sim D_0 e^{(\alpha_D s_2/k_B)}, \tag{1}$$

where the excess entropy is replaced with the two body entropy

$$s_2 = -2\pi\rho k_B \int \{g(r)\ln[g(r)] - [g(r)-1]\} r^2 dr. \tag{2}$$

In this way the accessible configurations are determined by the structural correlations.

Starting from Eq. (1) different scaling relations were formulated by Rosenfeld[48–50] and by Dzugutov.[51] Those relations were tested by computer simulation in different liquid systems.[48,52–59]

In particular the two body excess entropy of water was found to be connected to the structural anomaly of the liquid[59–62] and to the liquid-liquid transition.[59,63,64] In a detailed study of how the excess entropy behavior is related to the diffusion anomaly in water, it was found[59] that s_2 shows a good agreement with the trend of the diffusion coefficient in a large temperature and density range.

More recently the relation between s_2 and the dynamics of supercooled liquids in the framework of MCT was discussed in details with the support of computer simulation performed on different glass forming liquids.[65]

In analogy with what was found in the bulk phase of TIP4P water[66] here we study the two body excess entropy to make a further test of how s_2 can be used to predict the dynamical behavior of supercooled water. The investigation in a large range of temperature upon supercooling will show whether s_2 can give results comparable to the MCT and also it can predict the dynamical crossover in confined water. The two body entropy will be calculated for the sake of comparison both in confined and bulk SPC/E water.

The paper is structured as follows. In Sec. II we describe the model and the methods that we used in our simulations. In Sec. III we present the radial distribution functions of the confined free water and we compare it with the bulk functions. In Sec. IV we show the two body entropy as obtained from the RDF of the confined water and compare it with the analogous quantity for bulk water. We also show that both in bulk and confined water the behavior of the entropy is connected to the dynamical crossover. Sec. V is devoted to conclusions.

II. SIMULATION OF CONFINED WATER

We performed new molecular dynamics simulations of water confined in MCM-41 with the same model and methods used in previous work.[42] A silica pore is modeled to reproduce the properties of MCM-41. Inside a cubic silica cell of length $L = 4.278$ nm a cylindrical pore of diameter 1.5 nm was carved. At the end of the procedure at the surface of the pore there are bridging oxygens (bO) with two silicon neighbors and non-bridging oxygens (nO) with only one silicon neighbor. The nO were saturated with acidic hydrogens (aH). The axis of the cylindrical pore is assumed along the z-direction.

The water was simulated with the SPC/E potential. SPC/E is a three site model, where one site (O) represents the oxygen and the other two (H) the hydrogens. The interaction of the water sites (O, H) with the atoms of the substrate (Si, bO, nO, aH) is determined by an effective potential.[67] Periodic boundary conditions are applied to the cubic box.

The shifted force method was adopted with a cutoff at 0.9 nm for all the interactions. The size of the initial cubic box length was chosen by taking into account already the cutoff of the potentials. As in the previous work we use $N_w = 380$ water molecules to get an average density of 1.0 g/cm^3 in the inner part of the pore. We simulated temperatures ranging from $T = 300$ K to $T = 200$ K.

We simulated also the bulk water with the SPC/E potential. The molecular dynamics was performed with 512 molecules at the density of 1.0 g/cm^3, equivalent to the average density of the free water confined in the pore. The temperature range was from $T = 300$ K to $T = 190$ K. For bulk water the cutoff of the potentials was taken at 0.95 nm. For the Coulomb interactions we implemented the Ewald method and the Particle Mesh Ewald (PME) algorithm was used.

Both for confined and bulk water we used a time step of 1 fs.

The results presented here were obtained by using the parallel Gromacs package 4.5.5.[68] The equilibration is performed by means of the Berendsen thermostat. Production runs are done in the microcanonical ensemble.

III. ANALYSIS OF THE RADIAL DISTRIBUTION FUNCTIONS IN CONFINEMENT

In Fig. 1 we show the density profile calculated along the pore radius. A double layer of water is found close to the hydrophilic substrate. As discussed in previous work the water molecules that reside on the average in this double layer form hydrogen bonds with the bridging oxygens of the silica. This bound water shows a very slow dynamics with a subdiffusive regime at long times already at room temperature. Instead the water in the cylindrical region $0 < R < 0.55$ nm, the free water, shows a behavior similar to bulk water.[42]

As said above the calculation of the site-site radial distribution functions (RDFs) is not a straightforward task for a confined liquid, since excluded volume effects must be taken into account. It is known that from simulation we can calculate the average number $n_{ab}^{(2)}(r)$ of atoms (or sites) b that are found in a spherical shell at a distance r from an atom (or site) a. If $\Delta v(r)$ is the volume of the spherical shell we can calculate the *spherical* function

$$g_{ab}^{(s)}(r) = \frac{n_{ab}^{(2)}(r)}{n_b \cdot \Delta v(r)}, \tag{3}$$

where $n_b = N_b/V_c$ is the density of the atoms (or sites) b in the cell of volume V_c. This quantity represents the deviation of the distribution of the interacting particles with respect to the ideal gas distribution in the spherical shell. In applying Eq. (3) the normalization is performed by assuming a homogeneous distribution of non-interacting particles in all the directions. In a normal simulation cell with periodic boundary conditions applied in all the directions this is a good approximation and $g_{ab}^{(s)}(r)$ coincides with the ab-RDF. More in general it must be taken into account that the homogeneous distribution must be corrected with a function $g_u(r)$, the uniform distribution of ideal gas atoms inside a confined cell of

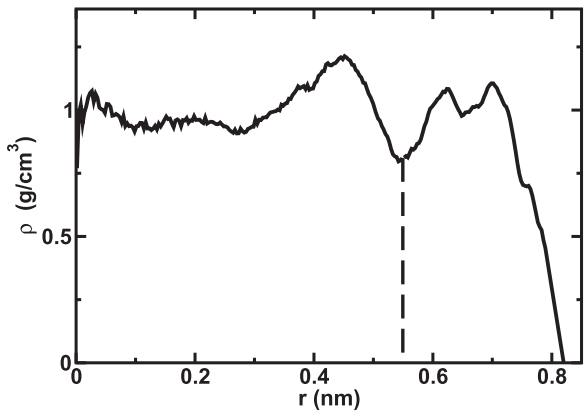

FIG. 1. Density profile along the pore radius.

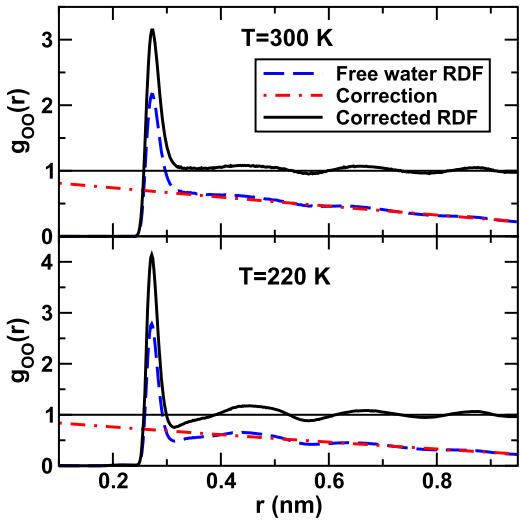

FIG. 2. Example of oxygen-oxygen RDF of free water. The black line represents the final result after the corrections of the RDF obtained from simulation (blue long dashed line) The red point dashed curve is the function used to perform the correction, see Eq. (4). Upper panel T = 300 K, lower panel T = 220 K.

simulation. Of course $g_u(r) = 1$ in the normal case, but for confined geometries $g_u(r)$ must be evaluated. In our case we must take into account the cylindrical geometry in which the water is confined. For this reason we adopt the same procedure used for extracting the RDF from the simulation of water in Vycor[46] and $g_u(r)$ is approximated as the Fourier transform of a cylindrical form factor. The site-site RDF can be obtained as

$$g_{ab}(r) = \frac{g_{ab}^{(s)}(r)}{f_c(r) \cdot g_u(r)}, \tag{4}$$

where $f_c(r)$ is a correction factor. This latter function accounts for the uncertainty in the volume and the presence of periodic boundary conditions along the z direction. By imposing that the RDF must go asymptotically to oscillate around the constant unity value it is possible to find that $f_c(r)$ is an asymptotic linear correction weakly dependent on r. In Fig. 2 we

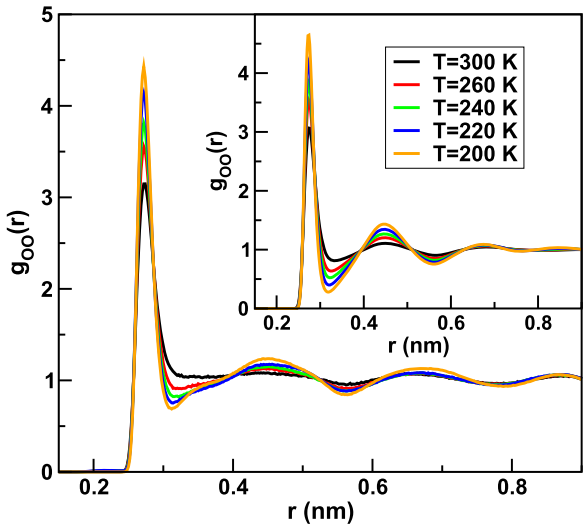

FIG. 3. Oxygen-oxygen RDF, free water in the main panel, bulk water in the inset at the temperatures indicated in the caption.

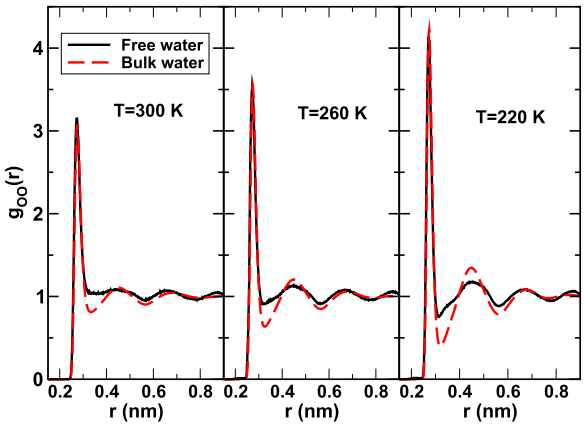

FIG. 4. Comparison of the oxygen-oxygen RDF of free water with bulk water at decreasing temperature as indicated in the panels.

report as examples $g_{OO}^{(s)}(r)$ as obtained from the simulation, the correction factors, and the final $g_{OO}(r)$ for $T = 300$ K and $T = 220$ K.

We computed the site-site RDF for the free water at decreasing temperatures from $T = 300$ K down to $T = 200$ K. In Figs. 3–6 we show $g_{OO}(r)$, $g_{OH}(r)$, and $g_{HH}(r)$ for few chosen temperatures as obtained after the corrections. We compare with the same functions of bulk SPC/E water at 1 g/cm^3.

By comparing $g_{OO}(r)$ of the confined free water in Fig. 3 with $g_{OO}(r)$ of the bulk reported in the inset of the figure we observe that the first minimum becomes shallower and fills in upon confinement in analogy with the case of confinement in Vycor glass.[46] The effect here however is more pronounced than for the Vycor case. The differences are shown more in detail in Fig. 4. The first peak of free water is sharp and high as bulk water, but the first minimum broadens with consequent more penetration between the second and the first shells. At decreasing temperature however the trend for free and bulk water is very similar, the position of the first minimum of free water shifts to lower distances as in the bulk, while the second maximum increases and it is located approximately at the same

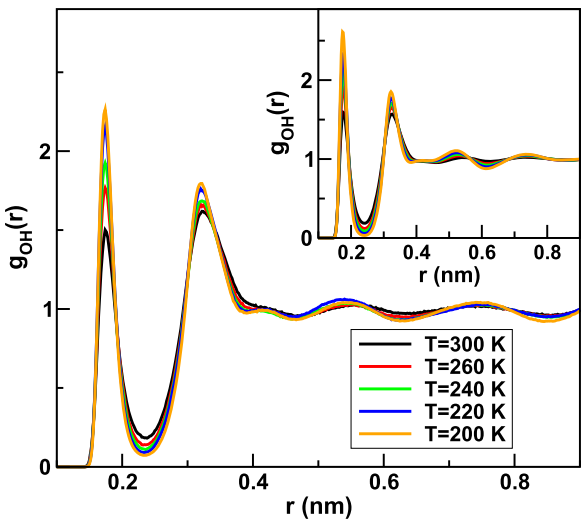

FIG. 5. Oxygen-hydrogen RDF, free water in the main panel, bulk water in the inset at the temperatures indicated in the caption.

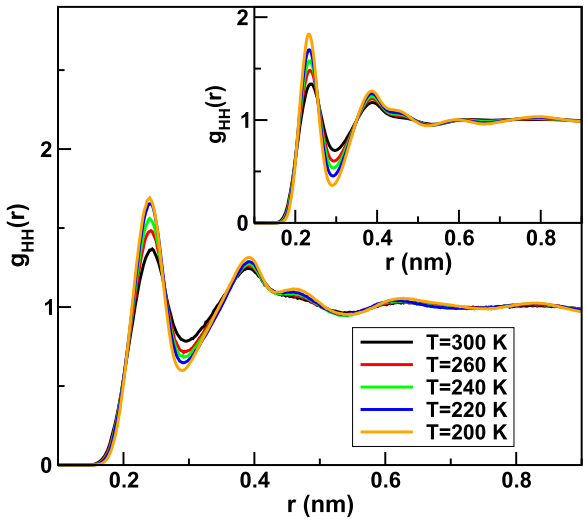

FIG. 6. Hydrogen-hydrogen RDF, free water in the main panel, bulk water in the inset at the temperatures indicated in the caption.

distance as in the bulk. The differences almost disappear after the second shell.

The main features of OH and HH RDF, reported in Figs. 5 and 6, respectively, are very similar to bulk water. The hydrophilic interaction induces a strong distortion of the layer of water close to the substrate but it perturbs less the hydrogen bond network in the middle of the pore. In Fig. 5 it is evident that there is practically no change in the OH structure. The first minimum of $g_{HH}(r)$ fills in as in the case of $g_{OO}(r)$. The oxygens and the hydrogens rearrange themselves also in confinement to form the HB network between the water molecules. Therefore in spite of the differences between OO and HH RDF in confinement the HB network in well preserved.

The evolution of the peaks of the RDF is very similar for free water in confinement and bulk water. In particular, looking back at the OO RDF we see that the first and the second peaks sharpen and the first minimum becomes deeper witnessing that

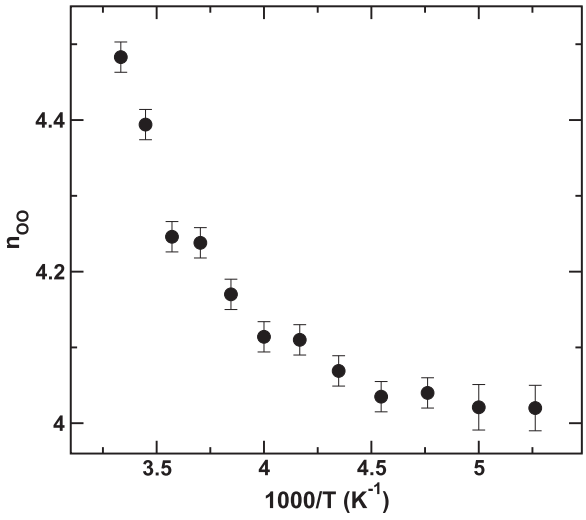

FIG. 7. First coordination number of the oxygens as function of inverse temperature for bulk water. The error bars are due to the uncertainty in locating the first minimum.

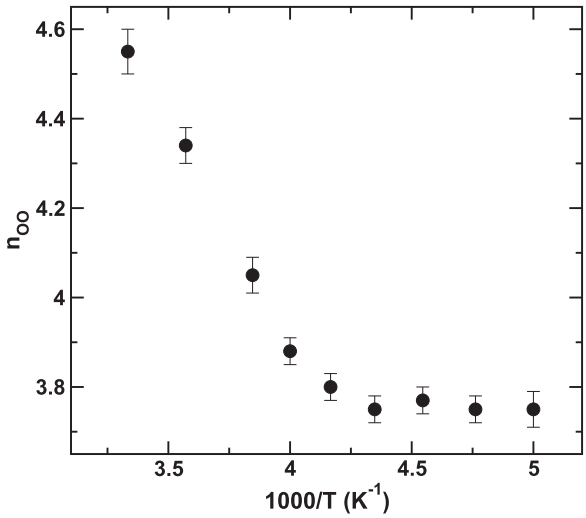

FIG. 8. First coordination number of the oxygens as function of inverse temperature for free water in MCM-41. The error bars are due to the uncertainty in locating the first minimum.

the system is evolving in a more ordered tetrahedral structure also in confinement. These features are present also in the experimental bulk RDF upon cooling.[69,70]

In this respect it is interesting to consider the coordination number of the first shell of $g_{OO}(r)$ defined as

$$n_{OO} = \frac{N_O}{V}\int_0^{r_1} 4\pi r^2 g_{OO}(r)\,, \tag{5}$$

where r_1 is the radius of the first shell and it coincides with the position of the first minimum.

The results are reported in Fig. 7 for bulk water and Fig. 8 for free water.

We observe the same trend for both cases. It is evident that the coordination number decreases upon cooling as expected since the first peak becomes more sharp and well separated from the second one. Around $T = 220$ K for bulk and free water we note a saturation toward an almost constant number. This is also a clear indication that upon cooling the system undergoes a crossover to a more ordered structure. We will see in Sec. IV that this behavior is connected to the fragile to strong crossover.

IV. TWO BODY ENTROPY AND THE FRAGILE TO STRONG CROSSOVER

We calculated in our previous simulations of water in MCM-41 the relaxation dynamics upon supercooling. We separated the contributions of the free and the bound water to the density self-intermediate scattering function. We found that while the dynamics of the bound water is almost completely frozen, the dynamics of free water is similar to bulk water. In particular the α relaxation time of free water follows the MCT prediction with an asymptotic power law divergence

$$\tau \sim (T - T_C)^{-\gamma}, \tag{6}$$

with $T_C = 195$ K and $\gamma = 3.2$.[42,43] In MCT the temperature T_C signs the ideal crossover from an ergodic to a non-ergodic regime. Upon decreasing temperature towards the asymptotic temperature T_C we observed that the relaxation time deviates from the fragile power law divergence to the strong behavior determined by activated processes and described by the Arrhenius formula

$$\tau \sim e^{E_a/k_B T}, \tag{7}$$

where E_a is the activation energy. For the free confined water it was found that $T_C = 195$ K and $T_L \approx 215$ K.[42]

For comparison in our calculations of bulk SPC/E water we found $T_C = 200$ K and a FSC at a temperature $T_L \approx 215$ K.

We consider now the relation between the two body excess entropy s_2 and the structural relaxation. This type of analysis was previously performed on TIP4P bulk water.[66] We consider that the relaxation processes are connected to the diffusion. Since the α relaxation time $\tau \sim 1/D$ we can assume

$$\frac{1}{\tau} = A e^{\alpha_\tau s_2/k_B}. \tag{8}$$

The connection between this equation and the MCT predictions has recently been demonstrated.[65]

The two body excess entropy can be derived from the RDF according to Eq. (2). We consider only the contribution of the oxygen-oxygen correlation since we study the translational part of the dynamics and the center of mass of the molecule can be identified with the oxygen.

By combining Eq. (6) with Eq. (8) we can hypothesize an asymptotic logarithmic divergence for the two body entropy in approaching T_C

$$s_2/k_B = a + b\ln(T - T_C)\,. \tag{9}$$

We started by testing Eq. (9) for our bulk SPC/E at density of 1.0 g/cm^3. s_2 calculated from the RDF discussed in Sec. III and the fit to the equation are shown in Fig. 9. The fit is performed with the value of $T_C = 200$ K.

For confined SPC/E free water s_2 calculated from the RDF of Sec. III is shown in Fig. 10 with the fit performed with $T_C = 195$ K.

As it is evident from both the figures s_2 as obtained empirically from the simulations predicts in both bulk and confined water an asymptotic power law divergence similar to the MCT predictions.

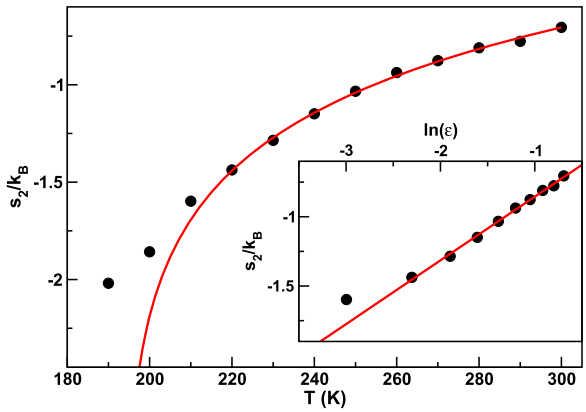

FIG. 9. Two body entropy of bulk SPC/E water at density 1.00 g/cm^3 as function of temperature. In the inset the same function reported versus $\ln(\epsilon)$ with $\epsilon = (T - T_C)/T_C$. In both panels the red curve is the fit to Eq. (9).

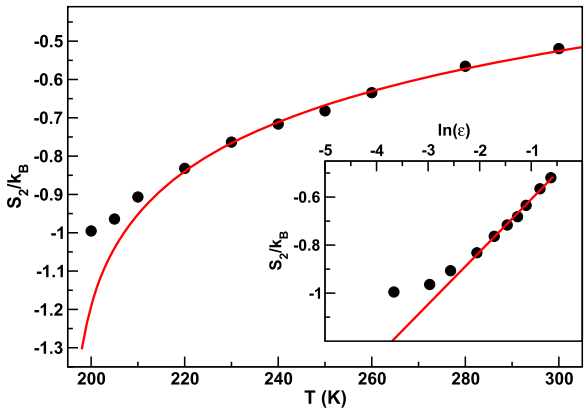

FIG. 10. Two body entropy of confined SPC/E free water at full hydration as function of temperature. In the inset the same function reported versus ln (ϵ) with $\epsilon = (T - T_C)/T_C$. In both panels the red curve is the fit to Eq. (9).

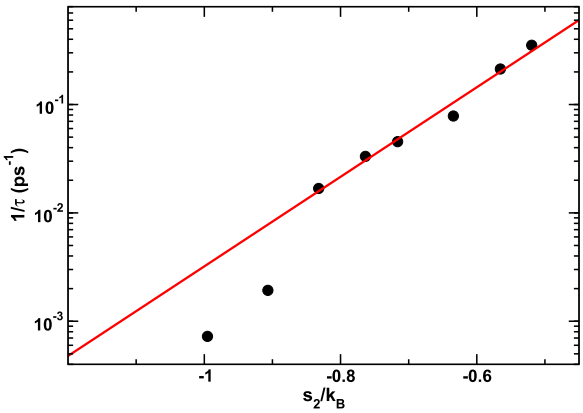

FIG. 12. Inverse of the α relaxation time as function of the two body entropy s_2 for confined free water. The red curve is the fit to Eq. (8).

As the temperature goes towards T_C s_2 deviates from the MCT behavior around the predicted fragile to strong crossover temperature in both cases. This confirms the important connection between dynamics and thermodynamics.

Coming back to the first coordination number n_{OO} shown in Fig. 7 for bulk water and Fig. 8 for free water, we observe that the saturation at low temperature starts very close to the FSC. This indicates that the FSC is closely related to the ordering taking place in water approaching the low density phase at the crossing of the Widom line both for bulk water and for free water confined in MCM-41.

To complete our test of this connection we use the values of τ as a function of T and we report those values as a function of s_2 at the corresponding temperature in Fig. 11 for bulk water and in Fig. 12 for confined water.

We perform the fit using the exponential prediction of Eq. (8) and we can see from both figures that this prediction is very well satisfied in the MCT regime for both bulk and confined free water showing no influence of finite size effect, see also Ref. 71. Deviations start to show up at the FSC.

The fact that s_2 is able to predict the relaxation dynamics and reproduce the MCT behavior on such a large temperature range indicates that the relevant entropic contribution to the dynamics at least down to the mild supercooled region is mainly due to the static pair correlations.[59] By cooling down below the FSC it is found that Eq. (8) is satisfied only in the region where MCT is valid but it fails when hopping effects intervene. It is possible that the inclusion of the three body and further terms could be necessary. But a possible influence of the many body terms in the excess entropy below the FSC will not change the usefulness of our results. We in fact show here that a measurable experimental quantity, $g(r)$, can indicate the location of the crossover from a fragile to a strong regime.

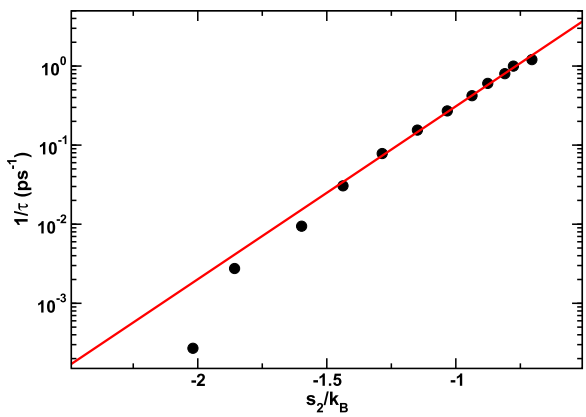

FIG. 11. Inverse of the α relaxation time as function of the two body entropy s_2 for bulk SPC/E water. The red curve is the fit to Eq. (8).

V. CONCLUSIONS

The study of the properties of confined water is a subject of major interest in many fields of research in physics and chemistry. From the point of view of understanding the anomalies of water the interest resides in the possibility of observing liquid water in a thermodynamic region that is more easily accessible in experiment when water is confined. How much the properties of water change under confinement or in contact with substrate is still a matter of debate and in this respect computer simulations can give new microscopic insights.

In this paper we presented results from the simulation of SPC/E water confined in a silica pore representing the MCM-41 material. Our study is a complement to our previous work on the dynamical properties. Our previous studies show that at least in hydrophilic environments the interaction with the substrate changes the behavior of water only in layers very close to the substrate. The liquid composed by the subset of water molecules close to the center of the pore, the free water, keeps much of the properties of bulk water. Upon supercooling we found in particular that the dynamics of the free water can be described in terms of MCT and that a fragile to strong crossover takes place similar to the bulk phase.

Now we derived the site radial distribution functions for the free water with the use of the finite volume corrections. By comparing the RDF of the free water upon supercooling with the RDF of bulk water at the same temperatures we find only mild changes in the oxygens-oxygens, the hydrogen-oxygen, and the hydrogen-hydrogen structures. The peaks are in the same positions but the first shell is less well defined in confinement, particularly for $g_{OO}(r)$. The trend in temperature, however, is the same as in bulk.

The oxygen-hydrogen structure, in particular, is really very similar to bulk water. So this evidences that the free water

preserves the hydrogen bond network with mild modifications with respect to the bulk.

The coordination number of the OO first shell clearly shows a change of trend at the fragile to strong crossover indicating a link of dynamics and structure and showing a more stable shell for the lowest temperatures.

We also calculated from the radial distribution functions of the oxygens the two body entropy. We find a logarithmic asymptotic divergence to the MCT T_C. This behavior is explained by assuming a Rosenfeld type of relation between the two body entropy and the α-relaxation. In approaching T_C the two body entropy changes its behavior in correspondence of the fragile to strong dynamic crossover temperature that we found in our previous study of the relaxation dynamics.[42,43] We found here that an analogous signature of the FSC in the two body entropy appears in bulk SPC/E water as it was found before in bulk TIP4P.[66]

Our results show that also in confined water, similar to the bulk, thermodynamic and structural properties are strictly related and that the two body entropy, that can be calculated from the RDFs, marks with good approximation the crossover from the fragile to the strong regime.

[1] J. C. Rasaiah, S. Garde, and G. Hummer, Ann. Rev. Phys. Chem. **59**, 713 (2008).
[2] P. Gallo, K. Amann-Winkel, C. A. Angell, M. A. Anisimov, F. Caupin, C. Chakravarty, E. Lascaris, T. Loerting, A. Z. Panagiotopoulos, J. Russo, J. A. Sellberg, H. E. Stanley, H. Tanaka, C. Vega, L. Xu, and L. G. M. Pettersson, Chem. Rev. **116**, 7463 (2016).
[3] S. Cerveny, F. Mallamace, J. Swenson, M. Vogel, and L. Xu, Chem. Rev. **116**, 7608 (2016).
[4] P. H. Poole, F. Sciortino, U. Essmann, and H. E. Stanley, Nature **360**, 324 (1992).
[5] S. Harrington, P. H. Poole, F. Sciortino, and H. E. Stanley, J. Chem. Phys. **107**, 7443 (1997).
[6] M. Yamada, S. Mossa, H. Stanley, and F. Sciortino, Phys. Rev. Lett. **88**, 195701 (2002).
[7] P. H. Poole, I. Saika-Voivod, and F. Sciortino, J. Phys.: Condens. Matter **17**, L431 (2005).
[8] D. Paschek, Phys. Rev. Lett. **94**, 217802 (2005).
[9] D. Corradini, M. Rovere, and P. Gallo, J. Chem. Phys. **132**, 134508 (2010).
[10] J. L. F. Abascal and C. Vega, J. Chem. Phys. **133**, 234502 (2010).
[11] V. Holten and M. Anisimov, Sci. Rep. **2**, 713 (2012).
[12] A. Nilsson and L. G. M. Pettersson, Chem. Phys. **389**, 1 (2011).
[13] O. Mishima, L. D. Calvert, and E. Whalley, Nature **314**, 76 (1985).
[14] K. Winkel, M. Elsaesser, E. Mayer, and T. Loerting, J. Chem. Phys. **128**, 044510 (2008).
[15] C. U. Kim, B. Barstow, M. V. Tate, and S. M. Gruner, Proc. Natl. Acad. Sci. U. S. A. **106**, 4596 (2009).
[16] K. Winkel, E. Mayer, and T. Loerting, J. Phys. Chem. B **115**, 14141 (2011).
[17] J. Palmer, R. Car, and P. Debenedetti, Faraday Discuss. **167**, 77 (2013).
[18] J. Palmer, F. Martelli, Y. Liu, R. Car, A. Z. Panagiotopoulos, and P. G. Debenedetti, Nature **510**, 385 (2014).
[19] P. H. Poole, R. K. Bowles, I. Saika-Voivod, and F. Sciortino, J. Chem. Phys. **138**, 034505 (2013).
[20] P. Gallo and F. Sciortino, Phys. Rev. Lett. **109**, 177801 (2012).
[21] H. E. Stanley, MRS Bull. **24**, 22 (1999).
[22] O. Mishima and H. E. Stanley, Nature **392**, 164 (1998).
[23] O. Mishima and H. E. Stanley, Nature **396**, 329 (1998).
[24] J. A. Sellberg, C. Huang, T. A. McQueen, N. D. Loh, H. Laksmono, D. Schlesinger, R. G. Sierra, D. Nordlund, C. Y. Hampton, D. Starodub, D. P. DePonte, M. Beye, C. Chen, A. V. Martin, A. Barty, K. T. Wikfeldt, T. M. Weiss, C. Caronna, J. Feldkamp, L. B. Skinner, M. M. Seibert, M. Messerschmidt, G. J. Williams, S. Boutet, L. G. M. Pettersson, M. J. Bogan, and A. Nilsson, Nature **510**, 381 (2014).
[25] P. Gallo, F. Sciortino, P. Tartaglia, and S.-H. Chen, Phys. Rev. Lett. **76**, 2730 (1996).
[26] F. Sciortino, P. Gallo, P. Tartaglia, and S.-H. Chen, Phys. Rev. E **54**, 6331 (1996).
[27] W. Götze, *Complex Dynamics of Glass-Forming Liquids: A Mode-Coupling Theory* (Oxford University Press, Oxford, 2009).
[28] R. Torre, P. Bartolini, and R. Righini, Nature **428**, 296 (2004).
[29] A. Dehaoui, B. Issenmann, and F. Caupin, Proc. Natl. Acad. Sci. U. S. A. **112**, 12020 (2015).
[30] M. De Marzio, G. Camisasca, M. Rovere, and P. Gallo, "Microscopic origin of the fragile to strong crossover in supercooled water: The role of activated processes," J. Chem. Phys. (to be published).
[31] A. Faraone, L. Liu, C.-Y. Mou, C.-W. Yen, and S.-H. Chen, J. Chem. Phys. **121**, 10843 (2004).
[32] L. Liu, S.-H. Chen, A. Faraone, C.-W. Yen, and C.-Y. Mou, Phys. Rev. Lett. **95**, 117802 (2005).
[33] Z. Wang, K. Ito, J. B. Leao, L. Harriger, Y. Liu, and S.-H. Chen, J. Phys. Chem. Lett. **6**, 2009 (2015).
[34] F. W. Starr, F. Sciortino, and H. E. Stanley, Phys. Rev. E **60**, 6757 (1999).
[35] L. Xu, P. Kumar, S. V. Buldyrev, S. H. Chen, P. H. Poole, F. Sciortino, and H. E. Stanley, Proc. Natl. Acad. Sci. U. S. A. **102**, 16558 (2005).
[36] P. Gallo and M. Rovere, J. Chem. Phys. **137**, 164503 (2012).
[37] P. Gallo, D. Corradini, and M. Rovere, J. Chem. Phys. **139**, 204503 (2013).
[38] M. De Marzio, G. Camisasca, M. Rovere, and P. Gallo, J. Chem. Phys. **144**, 074503 (2016).
[39] D. Corradini, P. Gallo, S. V. Buldyrev, and H. E. Stanley, Phys. Rev. E **85**, 051503 (2012).
[40] G. Franzese and H. E. Stanley, J. Phys.: Condens. Matter **19**, 205126 (2007).
[41] P. Gallo, D. Corradini, and M. Rovere, Nat. Commun. **5**, 5806 (2014).
[42] P. Gallo, M. Rovere, and S.-H. Chen, J. Phys. Chem. Lett. **1**, 729 (2010).
[43] P. Gallo, M. Rovere, and S.-H. Chen, J. Phys.: Condens. Matter **24**, 064109 (2012).
[44] P. Gallo, M. Rovere, and S.-H. Chen, J. Phys.: Condens. Matter **22**, 284102 (2010).
[45] P. Gallo, R. Pellarin, and M. Rovere, Europhys. Lett. **57**, 212 (2002).
[46] P. Gallo, M. Ricci, and M. Rovere, J. Chem. Phys. **116**, 342 (2002).
[47] P. Gallo, M. Rovere, M. Ricci, C. Hartnig, and E. Spohr, Philos. Mag. B **79**, 1923 (1999).
[48] Y. Rosenfeld, J. Phys.: Condens. Matter **11**, 5415 (1999).
[49] Y. Rosenfeld, Phys. Rev. A **15**, 2545 (1977).
[50] Y. Rosenfeld, Phys. Rev. E **62**, 7524 (2000).
[51] M. Dzugutov, Nature **381**, 137 (1996).
[52] B. S. Jabes, M. Agarwal, and C. Chakravarty, J. Chem. Phys. **132**, 234507 (2010).
[53] M. Agarwal, M. Singh, R. Sharma, M. P. Alam, and C. Chakravarty, J. Phys. Chem. B **114**, 6995 (2011).
[54] R. Sharma, M. Agarwal, and C. Chakravarty, Mol. Phys. **106**, 1925 (2008).
[55] J. Mittal, J. R. Errington, and T. M. Truskett, J. Chem. Phys. **125**, 076102 (2006).
[56] J. R. Errington, T. M. Truskett, and J. Mittal, J. Chem. Phys. **125**, 244502 (2006).
[57] A. Scala, F. W. Starr, E. L. Nave, F. Sciortino, and H. E. Stanley, Nature **406**, 166 (2000).
[58] Y. D. Fomin, V. N. Ryzhov, and N. V. Gribova, Phys. Rev. E **81**, 061301 (2010).
[59] M. E. Johnson and T. Head-Gordon, J. Chem. Phys. **130**, 214510 (2009).
[60] J. R. Errington and P. G. Debenedetti, Nature **409**, 318 (2001).
[61] J. Mittal, J. R. Errington, and T. M. Truskett, J. Phys. Chem. B **110**, 18147 (2006).
[62] F. Saija, A. M. Saitta, and P. V. Giaquinta, J. Chem. Phys. **119**, 3597 (2003).
[63] Z. Yan, S. V. Buldyrev, and H. E. Stanley, Phys. Rev. E **78**, 051201 (2008).
[64] P. Gallo, D. Corradini, and M. Rovere, Mol. Phys. **109**, 2969 (2011).
[65] M. K. Nandi, A. Banerjee, S. Sengupta, S. Sastry, and S. M. Bhattacharyya, J. Chem. Phys. **143**, 174504 (2015).
[66] P. Gallo and M. Rovere, Phys. Rev. E **91**, 012107 (2015).
[67] E. Spohr, C. Hartnig, P. Gallo, and M. Rovere, J. Mol. Liq. **80**, 165 (1999).
[68] B. Hess, C. Kutzner, D. V. der Spoel, and E. Lindahl, J. Chem. Theory Comput. **4**, 435 (2008).
[69] L. B. Skinner, C. Huang, D. Schlesinger, L. G. M. Pettersson, A. Nilsson, and C. J. Benmore, J. Chem. Phys. **138**, 074506 (2013).
[70] L. B. Skinner, C. J. Benmore, J. C. Neuefeind, and J. B. Parise, J. Chem. Phys. **141**, 214507 (2014).
[71] L. Berthier, G. Biroli, D. Coslovich, W. Kob, and C. Toninelli, Phys. Rev. E **86**, 031502 (2012).